Optimized Conditions for Catalytic Chemical Vapor Deposition of Vertically Aligned Carbon Nanotubes

M. Makenali[*], R. Ajeian, M. Tavakkoli, M. Nakhaee Badrabadi, S. Panahian Jand, and M. Zare

Thin Films Laboratory, School of Physics, Iran University of Science and Technology, Tehran, Islamic Republic of Iran

Abstract

Here, we have synthesized vertically aligned carbon nanotubes (VA-CNTs), using chemical vapor deposition (CVD) method. Cobalt and ethanol are used as the catalyst and the carbon source, respectively. The effects of ethanol flow rate, thickness of Co catalyst film, and growth time on the properties of the carbon nanotube growth are investigated. The results show that the flow rate of ethanol and the Co layer thickness play important roles on the length and the degree of alignment of the carbon nanotubes. High density VA-CNTs with forest-like structure are grown at a very low ethanol flow rate of 0.8 sccm, which is the optimized flow rate in our experiments. Therefore, the cost of synthesizing VA-CNTs is decreased by a low consumption of ethanol and utilizing the cheap CVD synthesis method. High density of small-sized catalyst particles is formed in the Co-catalyst thickness of 1 and 2nm, resulting in the growth of vertically aligned nanotubes. However, increasing the thickness of Co layer to 10 and 16 nm, leads to the growth of nanotubes parallel to the substrate with the spaghetti-like structure. The experiments reveal that enhancing the growth time from 5 to 120 min can mostly affect the uniformity and length of VA-CNTs.

Keywords: Vertically aligned carbon nanotubes; Ethanol flow rate; Co catalyst thickness; Growth time.

[*] Corresponding author: Tel: +989106042518; Fax: +982177240497; Email: Marzieh.Makenali@gmail.com

Introduction

Carbon nanotubes (CNTs) have been studied intensively because of their unique structural, mechanical and electrical properties [1-5], such as electron field emission, photoconductivity, spin coherent transport, and very high thermal conductivity. Vertically growth of CNTs with high density (forest-like structure) directly on a desired position of various substrates is highly important for many applications [6], and forest of vertically aligned CNTs has shown notable optical properties [7, 8]. Mizuno *et al.* [9] have reported that among all known materials, a forest-like structure of vertically aligned single-walled carbon nanotubes (VA-SWCNTs) behaves most similarly to a black body. For the synthesis of CNTs, chemical vapor deposition (CVD) methods may have priority to other techniques due to the ability of growth on a large-scale, and the easiness of controlling their structure. Alcohol vapor has been used as an effective carbon source for synthesizing SWCNTs by various groups [10-12] .Highly pure CNTs could be grown using ethanol as a low-cost carbon source by the method so-called alcohol catalytic chemical vapors deposition (ACCVD), which is expected to be a potential technique for the fabrication of electronic devices [13]. A multilayered catalyst structure has been used by many groups to improve the CNTs production at low temperatures [14, 15].

In this paper, we used a catalyst with the sandwich structure of Al/Co/Al on Si substrate. Then, we studied various factors, such as the effects of ethanol flow rate, thickness of catalyst, and growth time, on the properties of the VA-CNTs grown by ACCVD method using ethanol carbon source.

Materials and Methods

The CNTs were grown using ACCVD method with a quartz tube vacuum furnace. In our experiments, Si p-type (100) wafers were utilized as substrate. After routine solvent cleaning of substrates, a catalyst with the sandwich structure of Al (10 nm)/Co (1-16 nm)/Al (0.5 nm) was deposited by thermal evaporation under a base pressure of approximately 10^{-6} Mbar. A quartz crystal balance oscillator controlled thickness of the evaporated layers. The low-lying Al layer was used as buffer layer [16], which could also cause a decrease in the probability of catalyst sintering [15]. The Al top layer forms a stable alumina–catalyst interface and additionally stabilizes small Co clusters [15].

After deposition of the Al/Co/Al sandwich structure in a PVD-chamber, the substrates were transferred into the quartz tube of CVD reactor (with 2.5 cm diameter and 100 cm length), which was first evacuated using a rotary pump to a pressure of about 10^{-2} Mbar. Then, argon as carrier gas was introduced into the chamber at a flow rate of 200 sccm and the substrates were heated up to 650°C and held at this temperature for 15 min in order to form Co nanoparticles as nucleation centers. After the substrate treatment, ethanol vapor as a carbon source was immediately fed into the CVD reactor for 10 - 120 min at aforementioned temperature of 650°C. In the various experiments, the ethanol flow rate in the growth chamber changed from 0.1 - 1.5 sccm by varying the temperature of ethanol flask using a hot
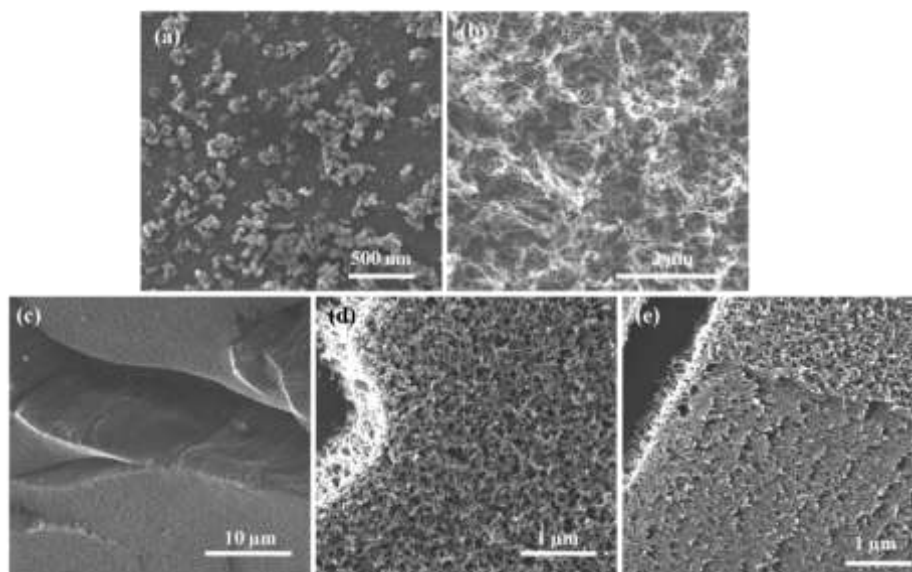
Figure 1. SEM images of CNTs grown with ethanol flow rate of (a) 0.1, (b) 0.3, (c) 0.8, and (d)-(e) 1.5 sccm.

plate. After growth, the ethanol gas flow was stopped, and, in the presence of argon flow, the substrate was left to cool down to room temperature.

The morphological aspect of the samples and the quality of CNT growth, including density, length, and orientation of them, were analyzed by scanning electron microscope (SEM) [TESCAN VEGA//]. Raman spectroscopic analysis of CNTs was carried out using the Raman Alimga Thermo Nicolet spectrometer with a laser wavelength of 532 nm under ambient conditions.

Results and Discussion

The effect of the ethanol vapor concentration on the properties of the CNTs grown in the CVD reactor was considered by varying ethanol flow rate. Therefore, while other variable conditions in this study were kept constant, i.e. Co thickness=1 nm in Al/Co/Al structure and growth time=45 min, the ethanol flow rates of 0.1, 0.3, 0.8, and 1.5 sccm were chosen by changing the temperature of the ethanol container accordingly.

SEM images of carbon nanostructures grown at the

various ethanol flow rates are shown in figure 1. As seen in this figure, for ethanol flow rate of 0.1 sccm no CNT growth was observed and just catalyst clusters or amorphous carbon would be created. When the ethanol flow rate was increased to 0.3 sccm, randomly oriented CNTs parallel to the substrates with spaghetti-like structure could be detected. By increasing ethanol flow rate to 0.8 sccm, vertically aligned CNTs with forest-like structure were observed. Ethanol flow rate of 1.5 sccm resulted in CNT growth in a direction parallel to the substrates mixed with vertically grown nanotube arrays. However, the length of these CNTs in comparison to the length of those grown in the flow rates of 0.3 and 0.8 sccm was significantly shorter.

At the growth temperature of about 650^0 C, the hydrocarbon will decompose to carbon atoms and smaller molecules. The diffusion of carbon atoms during the heat treatment can form carbon aggregations, which would also diffuse along with carbon atoms and smaller molecules. If diffusion of carbon atoms and aggregations on Al surface is faster than their escaping ratio on the Co perimeter, they can be accumulated at
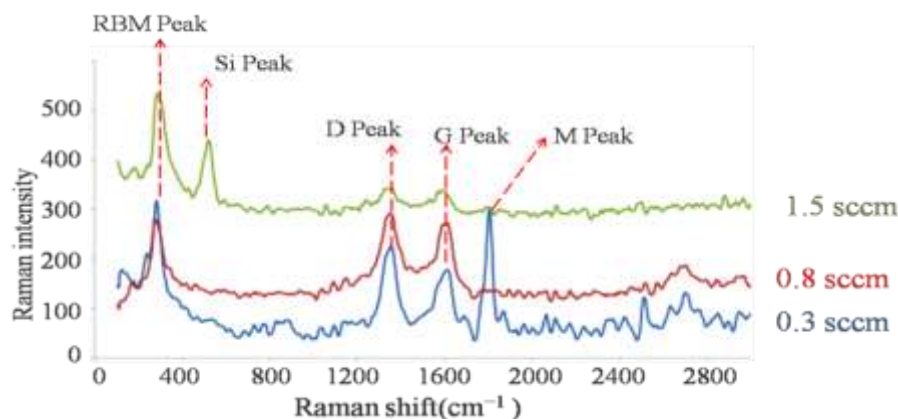

Figure 2. Raman spectra of CNTs grown with 0.3, 0.8 and 1.5 sccm flow rates of ethanol respectively.
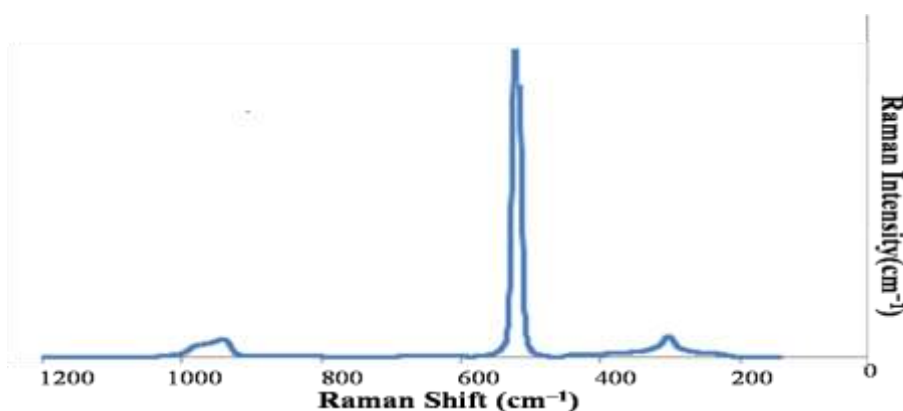

Figure 3. Raman spectra of pure Si substrate

the perimeter of Co nanoparticle to form CNTs [16].

Different ethanol flow rates result in different carbon fluxes on the substrate and, therefore, in various densities of the accumulated carbon at the perimeter of the Co nanoparticle. In our experiments, the accumulated carbon at the Co perimeter was not sufficient to commence the nucleation for CNT growth at ethanol flow rate of 0.1 sccm. By increasing ethanol flow rate to 0.3 sccm, carbon flux increased so that a higher density of the accumulated carbon at the perimeter of the Co nanoparticle was provided in order to form low density CNTs with spaghetti-like structure. As flow rate increased to 0.8 sccm, the collected carbon source at the perimeter of the Co nanoparticle could be enough to form highly dense vertically aligned CNTs with forest-like structure. In this study, ethanol flow rate of about 0.8 sccm was presented as a critical flow rate for emerging CNTs which were mostly aligned in a vertical direction, since by increasing the flow rate to 1.5 sccm, CNTs were also grown in various directions. At the flow rate of 1.5 sccm, precipitated carbon atoms and their aggregations may increase the probability of formation of CNT nucleation in various directions on the Co nanoparticles. This can result in CNTs grown in a direction parallel to the substrates mixed with vertically grown nanotube arrays. Furthermore, an increase in the flow rate may cause a Co catalyst poisoning and burning of CNTs [17]. This can lead to growth of CNTs with shorter length at flow rate of 1.5 sccm in comparison to their length at lower flow rates.

The Raman spectra of the CNTs grown by different flow rates are shown in figure 2. The strong peak at about 1590 cm^{-1} is attributed to the G-band of tangential mode of the graphitic structure while the peak around 1350 cm^{-1} is the D-band associated with the lattice defects process [18]. For the synthesized CNTs, the D-band signal intensity is stronger than that of the G-band, indicating considerable lattice defects. The Raman spectra of all the CNTs grown by ACCVD method in this investigation exhibit some peaks of radial breathing mode (RBM) in the range of 100 to 350 cm^{-1}, that shows the presence of single-walled CNTs with different diameters [19, 20].

The peak around 1800 cm^{-1} (M band) as a combination mode of the G band and RBM, and Si peak around 500 cm^{-1} are also seen at the spectra. By increasing ethanol flow rate from 0.3 to 1.5 sccm, the intensity of Raman spectra of CNTs grown decreased that can be attributed to increase in the amorphous carbon amounts. In accordance with figure 3, the peaks of Raman spectrum of silicon substrate are observed near frequencies of 300, 500 and 900 cm^{-1}; however, the prominent peak is at 500 cm^{-1}. In this experiment, the

peak of 500 cm^{-1} is only seen in a Raman spectrum of synthesized CNTs with the flow rate of 1.5 sccm. For other samples in this work, this peak is vanished as the density of CNTs, as an appropriate light absorber, increases. Furthermore, this can show that the peak of about 280 cm^{-1}; which is seen in all Raman spectra of grown CNTs, is not related to the Si substrate. This peak is attributed to the RBM peak of CNTs, which shows the existence of some single walled CNTs among the synthesized nanotubes in this research.

In other researches [16, 21-23], the ethanol flow rate for synthesizing CNTs by ACCVD method is dramatically higher, even more than 50 fold, compared to our work in this paper. One of the drawbacks of this work due to lattice defects is the D-band signal intensity, which is stronger than that of the G-band in all Raman spectra. In addition, the other experiments [21-23] have been done with comparatively higher growth temperature than 650°C, which we have used for CNTs growth with ACCVD method. Raising the temperature in our experiments can result in less amorphous carbon, and highly pure CNTs [13, 15, 17, 21].

In order to study the effect of thickness of catalyst with the sandwich structure of Al (10 nm)/Co/Al (0.5 nm) on the properties of the CNT growth, Co catalyst film thickness was changed from 1 to 16 nm while other variable conditions were kept constant, i.e. growth time ~ 45 min and ethanol flow rate ~ 0.8 sccm. The SEM images of Al/Co/Al catalysts in the various Co thicknesses of 1, 2, 10, and 16 nm, which were annealed at 650°C, are shown in figure 4. The mismatch of the thermal expansion coefficients of the catalyst and Si substrate causes that the catalyst heating breaks the catalyst layer into the small islands or nanoparticles [24, 25].

In addition, similar to the results of the other groups [24, 26-28], as figure 4 reveals, the island size depends on the thickness of the initial Co film. It can be seen that the density of the catalyst islands decreases, while the size of catalyst islands increases by raising the thickness of the Co layer. The catalyst islands are responsible for the CNT growth, and the key parameter to the growth of vertically aligned CNTs is to synthesize highly dense catalyst particles with small sizes [6, 15, 29]. In other words, the highly dense small-sized catalyst nanoparticles provide growing CNTs with high density. Their outermost walls interact via van der Waals forces with neighboring CNTs [30], resulting in a very dense forest-like vertically aligned CNTs.

Figure 5 shows SEM images of the CNTs grown with the different Co catalyst thicknesses. Similar forest-like VA-CNT arrays were grown on the basis of the catalysts with the Co thicknesses of 1 and 2 nm, in

which the high-density small-sized catalyst particles are formed. However, by increasing the Co thickness from 1 to 2 nm, the average length of the CNTs decreased from about 15 to 10.5 μm. As the Co thickness increased to 10 and 16 nm, CNTs emerged with spaghetti-like structure and their length reached to about 1μm. Nevertheless as figure 6 shows, for Co thickness of 16 nm, growth of forest-like structure of CNTs with

the length of about 6 μm is also observed in some parts. The CNT growth with mix of forest-like and spaghetti-like structures, can be seen on the catalyst layer with Co thickness of 16 nm, and it is attributed to the nonuniform fragmentation of the catalyst layer with Co thickness of 16 nm during annealing (figure 4) and change in shape and size of catalyst particles during CNT growth [26, 31].

As the catalyst thickness and the catalyst particle size increases, the density and length of the CNTs reduces. This reduction can be related to catalyst activity diminution, which decreases the growth rate [32, 33].
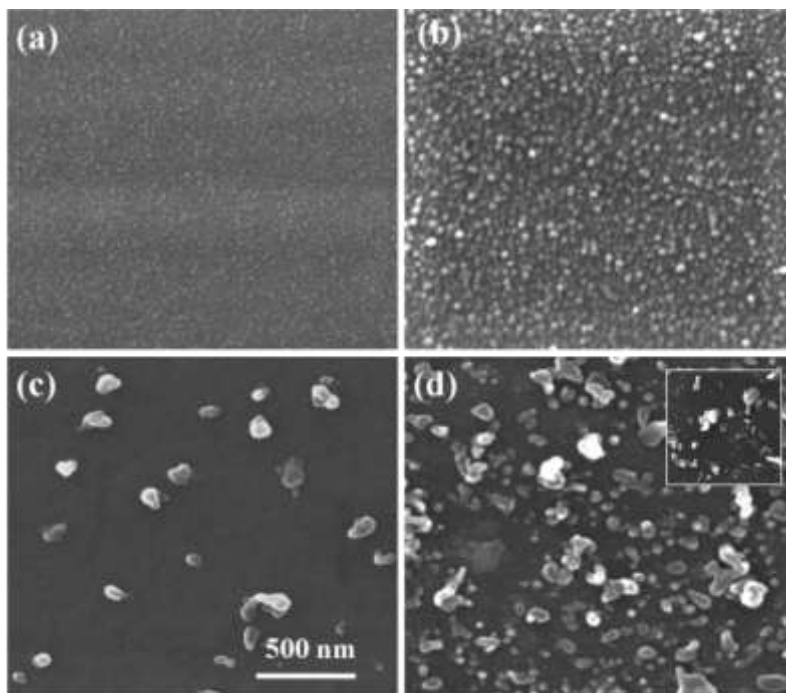
Figure 4. SEM images of the catalyst layer with the sandwich structure of Al/Co/Al on Si substrate, annealed at 650°C, in the various Co thicknesses of (a) 1nm, (b) 2nm, (c) 10nm, and (d) 16nm.
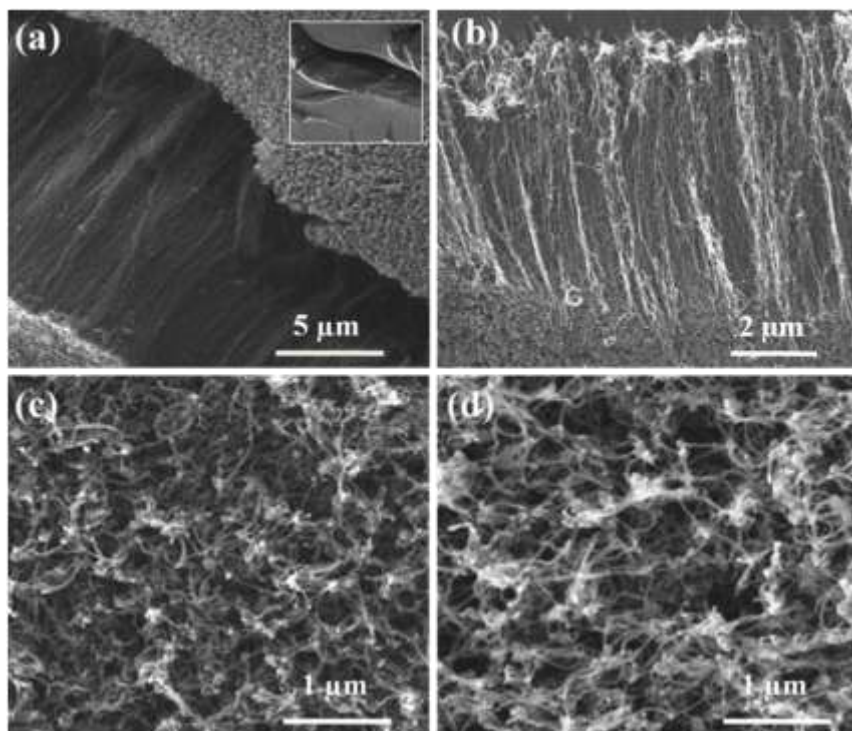
Figure 5. SEM images of CNTs grown with different Co thicknesses of (a, and its inset) 1nm, (b) 2 nm, (c) 10 nm, and (d) 16 nm.

As Figure 7 shows, there are no significant differences between the Raman spectra of CNTs grown with 1 and 2 nm Co thicknesses film. Also the spectra of CNTs grown on the catalysts with 10 and 16 nm are similar.
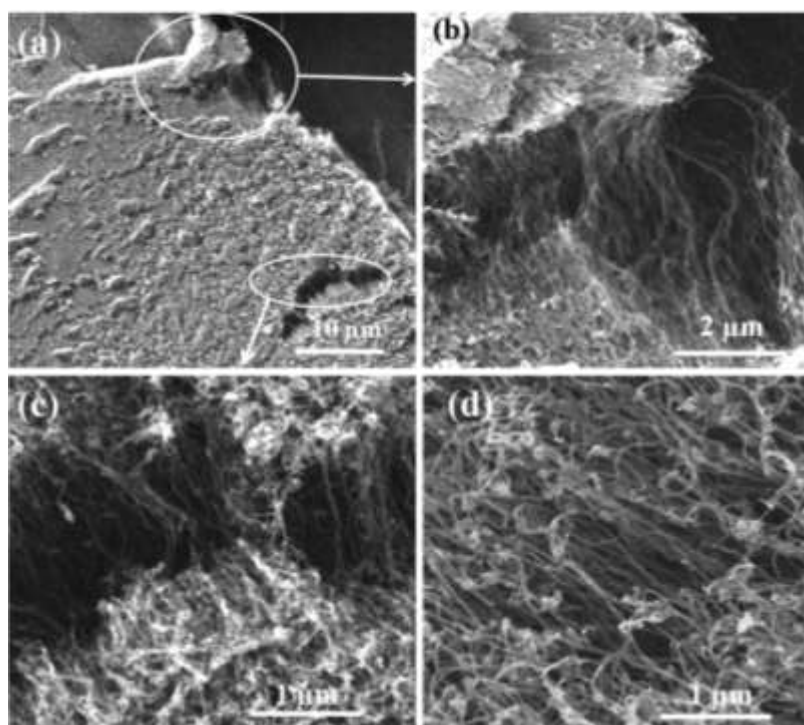
Figure 6. (a) SEM image of forest-like structure of CNTs grown with Co thickness of 16 nm. (b) The zoomed view of upper ellipsoid in (a). (c) The zoomed view of lower ellipsoid in (a). (d) Forest-like structure of CNTs grown from another section of the sample with Co thickness of 16 nm.

But by increasing the Co thickness from 1 and 2 to 10 and 16 nm, Raman intensity of CNTs grown decreased that can be attributed to increase in amorphous carbon amounts. When the Co thickness varies from 1 to 16 nm, the nearly similar RBM modes indicate almost constant diameter distribution and purity of the nanotubes. Therefore, varying the catalyst thickness mainly affects the degree of alignment and the length of

the CNTs synthesized at the mentioned conditions.

In order to investigate the effect of growth time on the properties of the synthesized CNTs, the time interval in which ethanol vapor flows into the chamber were set to 5, 10, 30, 45, 100, and 120 min while keeping all other parameters constant at the optimum (Co thickness ~ 1 nm and ethanol flow rate ~ 0.8 sccm). Figure 8 shows the Raman spectra of CNTs grown at different
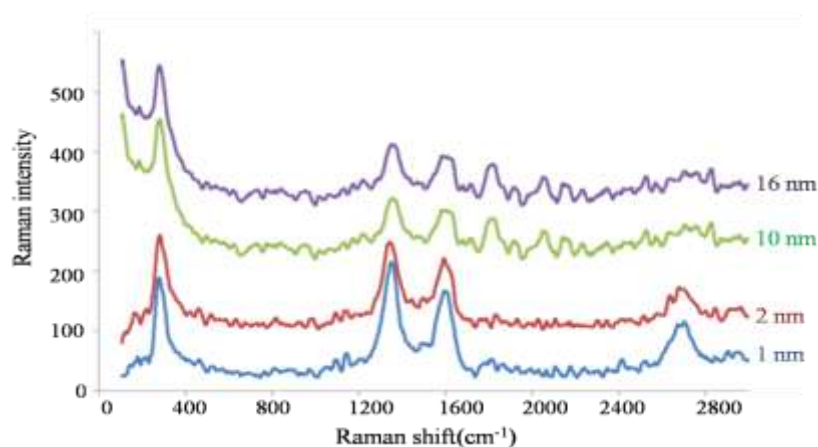
Figure 7. Raman spectra of CNTs grown with 1, 2, 10, and 16 nm of Co thicknesses layer respectively.
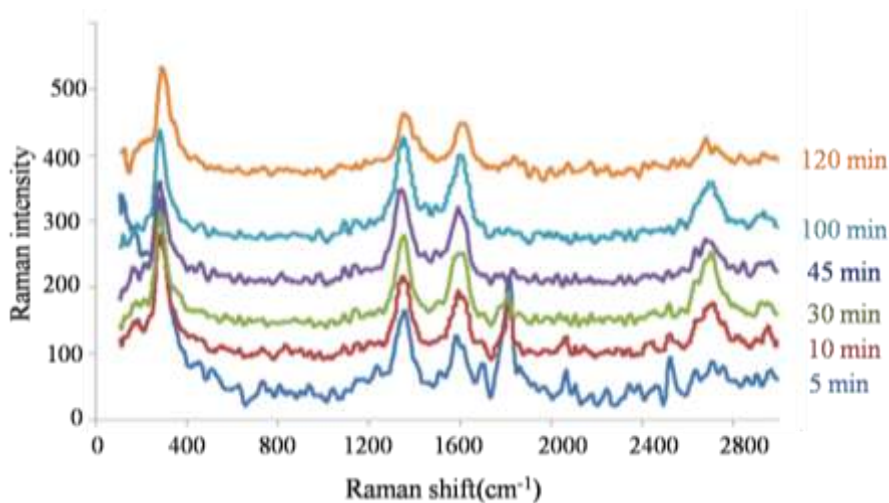
Figure 8. Raman spectra of CNTs grown at different growth times. Curves show the Raman spectra with 5, 10, 30, 45, 100 and 120 min of growth times respectively.
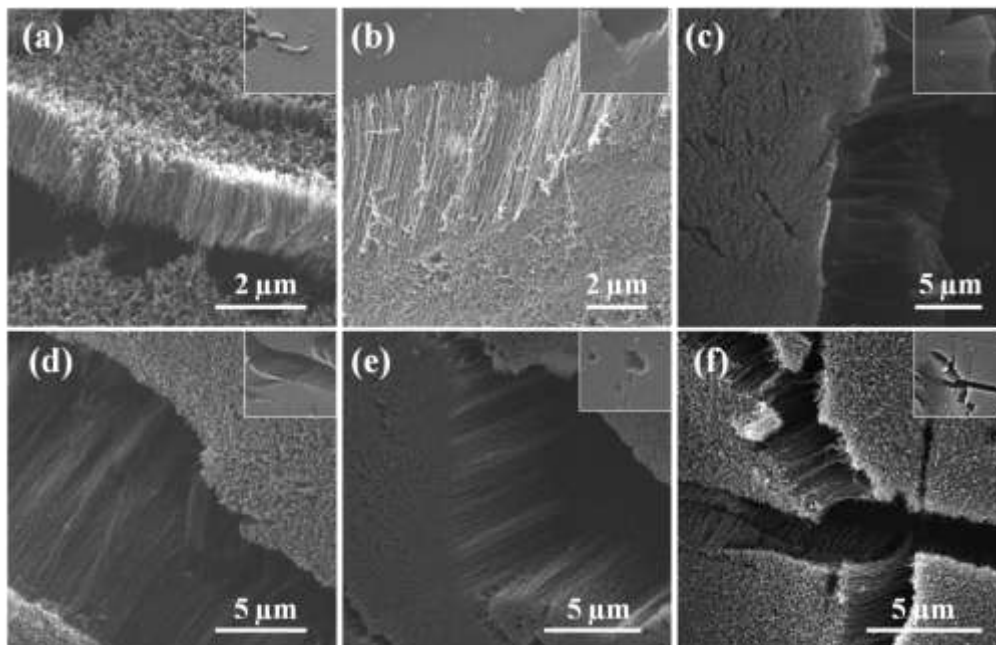
Figure 9. SEM micrograph of VA-CNTs grown at growth times of (a and its inset) 5 min, (b and its inset) 10 min, (c and its inset) 30 min, (d and its inset) 45 min, (e and its inset) 100 min, and (f and its inset) 120 min.

time intervals. The results indicate that there are no considerable differences among the Raman spectra of CNTs with various growth times from 5 to 100 min, but by increasing growth time to 120 min Raman intensity decreased.

I_D/I_G ratio is nearly constant for the different deposition times, resulting in CNTs with nearly similar structural quality.

Figure 9 shows SEM micrograph of vertically aligned CNTs grown at different time intervals. By increasing the growth time from 5 to 30 and to 45 min, the length of the CNTs reached from 2.5 to 10.5 and to 15 µm respectively. However, enhancing the growth time to 100 and to 120 min decreased the length of the CNTs to about 7 and to 4.5 µm respectively.

As the deposition time increases, the carbonization or

oxidation of the catalyst might cause the formation of the diffusion barrier layer around the catalyst [33-35] that reduces the CNTs growth rate. Furthermore, as the thickness of the CNT mat on the catalyst film increases, the mat can begin to act as a barrier, which reduces the supply of the ethanol to the catalyst below. This reduction can cause a decrease in the growth rate [36].

Decrease in the length of the CNTs as a result of a longer growth times is unclear. However, this can be attributed to the presence of excess oxygen in the CVD chamber, due to insufficient oxygen pumping, which hinders growth by reducing the catalyst activity, and can also oxidize the topmost portion of the mat [36-39].

A possible reason for the virtually slow growth rate of the CNTs grown by ACCVD method is that pure ethanol does not supply the proper balance of carbon, hydrogen, and oxygen. A number of groups [40-43] have reported that the proper carbon-hydrogen-oxygen balance is critical to the synthesis of millimeter-long VA-CNTs films. Therefore, the optimization of the aforementioned balance may significantly increase the length of the synthesized VA-CNTs.

Conclusions

In this study, the optimum conditions for synthesis of VA-CNTs using ACCVD method is investigated as a function of ethanol flow rate, Co catalyst thickness, and growth time. It is found that the highly dense structure of small-sized catalyst nanoparticles as well as sufficiently accumulated carbon at the perimeter of Co nanoparticles are the key factors to the growth of VA-CNTs. In our experiments, the very low ethanol flow rate of 0.8 sccm and 1 nm thick Co annealed at 650˚C are provided in order to grow high density VA-CNTs with forest-like structure. In the optimum conditions of ethanol flow rate (0.8 sccm) and Co thickness (1nm), the VA-CNTs mat on the substrate becomes more uniform as the growth time increases from 10 to 120 min. However, the growth time of 45 min results in the longest CNTs. CNTs grown in this research have similar ratio of I_D/I_G, indicating all samples have similar defects, which is attributed to the relatively low growth temperature of 650˚C.

References

1. Baughman R.H., Zakhidov A.A. and de Heer W.A. Carbon Nanotubes–the Route Towards Applications. *Science*. **297**: 787-792 (2002).

2. Wong E.W., Sheehan P.E. and Lieber C.M. Nanobeam Mechanics: Elasticity, Strength and Toughness of Nanorods and Nanotubes. *Science*. **277**: 1971-1975 (1997).

3. Yu M.F., Files B.S., Arepalli S. and Ruoff R.S. Tensile Loading of Ropes of Single Wall Carbon Nanotubes and Their Mechanical Properties. *Phys. Rev. Lett.* **84**: 5552-5555 (2000).

4. Odom T.W., Huang J.L., Kim P. and Lieber C.M. Atomic Structure and Electronic Properties of Single-Walled Carbon Nanotubes. *Nature*. **391**: 62-64 (1998).

5. Wildoer J.W.G., Venema L.C., Rinzler A.G., Smalley R.E. and Dekker C. Electronic Structure of Atomically Resolved Carbon Nanotubes. *Nature*. **391**: 59-62 (1998).

6. Rizzo A., Rossi R., Signore M.S., Piscopiello E., Capodieci L., Pentassuglia R., Dikonimos T. and Giorgi R. Effect of Fe Catalyst Thickness and C_2H_2/H_2 Flow Rate Ratio on the Vertical Alignment of Carbon Nanotubes Grown by Chemical Vapor Deposition. *Diam. Relat. Mater.* **17**: 1502-1505 (2008).

7. Cao A., Zhang X., Xu X., Wei B. and Wu D. Tandem Structure of Aligned Carbon Nanotubes on Au and its Solar Thermlal Absorption. *Sol Energ .Mat. Sol. C.* **17**: 481-486(2002).

8. Xi J.Q., Schubert M.F., Kim J.K., Schubert E.F., Chen M, Lin S.Y., Liu W. and Smart J. Optical Thin-Film Materials with Extremely Low Refractive Index for Broad-Band Elimination of Fresnel Reflection. *Nat Photonics*. **1**: 176-179 (2007).

9. Mizuno K., Ishii J., Kishida H., Hayamizu Y., Yasuda S., Futaba D.N., Yumura M. and Hata K. A Black Body Absorber from Vertically Aligned Single-Walled Carbon Nanotubes. *P. Natl. Acad. Sci. USA*. **106**: 6044-6047 (2009).

10. Okazaki T. and Shinohara H. Synthesis and Characterization of Single-Wall Carbon Nanotubes by Hot-Filament Assisted Chemical Vapor Deposition. *Chem. Phys. Lett.* **376**: 606-611 (2003).

11. Chiashi S., Murakami Y., Miyauchi Y. and Maruyama S. Cold Wall CVD Generation of Single-Walled Carbon Nanotubes and in Situ Raman Scattering Measurements of the Growth Stage. *Chem. Phys. Lett.* **386**: 89-94 (2004).

12. Nishide D., Kataura H., Suzuki S., Okubo O. and Achiba Y. Growth of Single-Wall Carbon Nanotubes from Ethanol Vapor on Cobalt Particles Produced by Pulsed Laser Vaporization. *Chem. Phys. Lett.* **392**: 309-313 (2004).

13. Maruyama S., Kojima R., Miyauchi Y., Chiashi S. and Kohno M. Low-Temperature Synthesis of High-Purity Single-Walled Carbon Nanotubes from Alcohol. *Chem. Phys. Lett.* **360**: 229-234 (2002).

14. Cantoro M., Hofmann S., Pisana S., Scardaci S., Parvez A., Ducati C., Ferrari A.C., Blackburn A.M. , Wang K.Y. and Robertson J. Catalytic Chemical Vapor Deposition of Single-Wall Carbon Nanotubes at Low Temperatures. *Nano. Lett.* **6**: 1107-1112 (2006).

15. Zhao Y., Huang D. and Saito Y. A Temperature Window for Ethanol Chemical Vapor Deposition of a Carbon Nanotube Array Catalyzed by Co Particles. *Nanotechnology*. **18:** 1-6 (2007).

16. Hahm M.G., Kwon Y.K., Lee E, Ahn C.W. and Jung Y.J. Diameter Selective Growth of Vertically Aligned Single Wall Carbon Nanotubes and Study on Their Growth Mechanism. *J. Phys .Chem*. C. **112**: 10418-10422 (2008).

17. Unalan H.E. and Chhowalla M. Investigation of Single-Walled Carbon Nanotube Growth Parameters using Alcohol Catalytic Chemical Vapour Deposition.

Nanotechnology. **16**: 2153-2163 (2005).

18. Li W., Zhang H., Wang C., Zhang Y., Xu L., Zhu K. and Xie S. Raman Characterization of Aligned Carbon Nanotubes Produced by Thermal Decomposition of Hydrocarbon Vapor. *Appl. Phys .Lett*. **70**: 2684-2686 (1997).

19. Saito R., Takeya T., Kimura T., Dresselhaus G. and Dresselhaus M.S. Raman Intensity of Single-Wall Carbon Nanotubes. *Phys. Rev. B*. **57**: 4145-4153 (1998).

20. Dresselhaus M.S., Dresselhaus G., Saito R. and Jorio A. Raman Spectroscopy of Carbon Nanotubes. *Phys. Rep*. **409**: 1-53 (2005).

21. Azam M.A., Mohamed M.A., Shikoh E. and Fujiwara A. Thermal Degradation of Single-Walled Carbon Nanotubes during Alcohol Catalytic Chemical Vapor Deposition Process. *Jpn. J. Appl. Phys*.**49**: 02BA04−1- 02BA04−6 (2010).

22. Inami N., Mohamed M.A., Shikoh E. and Fujiwara A. Synthesis-Condition Dependence of Carbon Nanotube Growth by Alcohol Catalytic Chemical Vapor Deposition method. *Sci. Technol. Adv. Mat*. **8**: 292-295 (2007).

23. Xiang R., Einarsson E., Okabe H., Chiashi S., Shiomi J. and Maruyama S. Patterned Growth of High-Quality Single-Walled Carbon Nanotubes from Dip-Coated Catalyst. *Jpn. J. Appl .Phys*. **49**: 02BA03-02BA03 (2010).

24. Bower C., Zhou O., Zhu W., Werder D.J. and Jin S. Nucleation and Growth of Carbon Nanotubes by Microwave Plasma Chemical Vapor Deposition. *Appl. Phys. Lett* .**77:** 2767-2769 (2000).

25. Merkulov V.I., Lowndes D.H., Wei Y.Y., Eres G. and voelkl E. Patterned Growth of Individual and Multiple Vertically Aligned Carbon Nanotubes. *Appl. Phys. Lett*. **76**: 3555-3557 (2000).

26. Chhowalla M., Teo K. B. K., Ducati C., Rupesinghe N. L., Amaratunga G. A. J., Ferrari A. C., Roy D.,Robertsonet J. and Milne W.I. Growth Process Conditions of Vertically Aligned Carbon Nanotubes Using Plasma Enhanced Chemical Vapor Deposition. *J .Appl. Phys*. **90**: 5308-5317 (2001).

27. Wei S., Kang W.P., Davidson J.L. and Huang J.H. Aligned Carbon Nanotubes Fabricated by Thermal CVD at Atmospheric Pressure Using Co as Catalyst with NH$_3$ as Reactive Gas. *Diam. Relat. Mater*. **15**: 1828-1833 (2006).

28. Wang Y., Luo Z, Li B. and Ho P.S. Comparison Study of Catalyst Nanoparticle Formation and Carbon Nanotube Growth: support, effect. *J. Appl .Phys*. **101**: 1-8 (2007).

29. Kanzow H. and Ding A. Formation Mechanism of Single-Wall Carbon Nanotubes on Liquid- Metal Particles. *Phys. Rev. B*. **60**: 11180-11186 (1999).

30. Fan S., Chapline M.G., Franklin N.R., Tombler T.W., Cassell A.M. and Dai H. Self-Oriented Regular Arrays of Carbon Nanotubes and Their Field Emission Propertie. *Science*. **283**: 512-514 (1999).

31. Srivastava K., Vankar V.D. and kumar V. Growth and Microstructures of Carbon Nanotube Films Prepared by Microwave Plasma Enhanced Chemical Vapor Deposition Process. *Thin Solid Films*. **515**: 1552-1560 (2006).

32. Hofmann S., Cantoro M., Kleinsorge B., Casiraghi C., Parvez A., Robertson J. and Ducati C. Effects of Catalyst Film Thickness on Plasma-Enhanced Carbon Nanotube Growth. *J. Appl .Phys*. **98**: 034308-03408 (2005).

33. Patole S. P., Kim H., Choi J., Kim Y., Baik S. and Yoo J.B. Kinetics of Catalyst Size Dependent Carbon Nanotube Growth by Growth Interruption Studies. *Appl. Phys .Lett*. **96**: 1-3 (2010).

34. Wang Y.Y., Tang G.Y., Koeck F.A.M., Brown B., Garguilo J.M. and Nemanich R.J. Experimental Studies of the Formation Process and Morphologies of Carbon Nanotubes with Bamboo Mode Structures. *Diam. Relat .Mater*. **13**: 1287-1291 (2004).

35. Pal S. K., Talapatra S., Kar S., Vajtai R., Ci L., Borca-Tasciuc T., Schadler L. and Ajayan P. M. Time and Temperature Dependence of Multi-Walled Carbon Nanotube Growth on Inconel 600. *Nanotechnology*. **19**: 1-6 (2008).

36. Einarsson E., Edamura T., Murakami Y., Igarashi Y. and Maruyama S. A Growth Mechanism for Vertically Aligned Single-Walled Carbon Nanotubes, *Therm. Sci*. **12**: 77-78 (2004).

37. Einarsson E., Murakami Y., Kadowaki M. and Maruyama S. Growth Dynamics of Vertically Aligned Single-Walled Carbon Nanotubes from in Situ Measurements. *Carbon*. **46**: 923-930 (2008).

38. Maruyama S., Einarsson E., Murakami Y. and Edamura T. Growth Process of Vertically Aligned Single-Walled Carbon Nanotubes. *Chem. Phys. Lett*. **403**: 3-20 (2005).

39. Duong H. M., Einarsson E., Okawa J., Xiang R. and Maruyama S. Thermal Degradation of Single-Walled Carbon Nanotubes. *Jpn J. Appl. Phys*. **47**: 1994-1999 (2008).

40. Hata K., Futaba D.N., Mizuno K., Namai T., Yumura M. and Iijima S. Water-Assisted Highly Efficient Synthesis of Impurity-Free Single-Walled Carbon Nanotubes. *Science*. **306**: 1362-1364 (2004).

41. Noda S., Hasegawa K., Sugime H., Kakehi K., Zhang Z., Maruyama S. and Yamaguchi Y. Millimeter-Thick Single-Walled Carbon Nanotube Forests: Hidden Role of Catalyst Support. *Jpn. J. Appl. Phys*. **46**: 399-401 (2007).

42. Zhang G., Mann D., Zhang L., Javey A., Li Y., Yenilmez E., Wang Q., McVittie J. P., Nishi Y., Gibbons J. and Dai H. Ultra-High-Yield Growth of Vertical Single-Walled Carbon Nanotubes: Hidden Roles of Hydrogen and Oxygen. *P. Natl. Acad. Sci. USA*. **102**: 16141-16145 (2005).

43. Xu Y.Q., Flor E, Kim M. J., Behrang H., Schmidt H. and Smalley R.E. Vertical Array Growth of Small Diameter Single-Walled Carbon Nanotubes. *J. Am. Chem .Soc*. **128**: 6560-6561 (2006).